

Ultraviolet Detection of Interstellar $^{12}\text{C}^{17}\text{O}$ and the CO Isotopomeric Ratios toward X Persei

Yaron Sheffer¹, David L. Lambert², and S. R. Federman¹

ABSTRACT

We report the detection of fully resolved absorption lines of $A-X$ bands from interstellar $^{12}\text{C}^{17}\text{O}$ and $^{12}\text{C}^{18}\text{O}$, through high-resolution spectroscopy of X Per with the Space Telescope Imaging Spectrograph³. The first ultraviolet measurement of an interstellar $^{12}\text{C}^{17}\text{O}$ column density shows that its isotopomeric ratio is $^{12}\text{C}^{16}\text{O}/^{12}\text{C}^{17}\text{O} = 8700 \pm 3600$. Simultaneously, the second ultraviolet detection of interstellar $^{12}\text{C}^{18}\text{O}$ establishes its isotopomeric ratio at 3000 ± 600 . These ratios are about five times higher than local ambient oxygen isotopic ratios in the ISM. Such severe fractionation of rare species shows that both $^{12}\text{C}^{17}\text{O}$ and $^{12}\text{C}^{18}\text{O}$ are destroyed by photodissociation, whereas $^{12}\text{C}^{16}\text{O}$ avoids destruction through self-shielding. This is to be contrasted with our ratio of $^{12}\text{C}^{16}\text{O}/^{13}\text{C}^{16}\text{O} = 73 \pm 12$ toward X Per, which is indistinguishable from $^{12}\text{C}/^{13}\text{C}$, the result of a balance between photodissociation of $^{13}\text{C}^{16}\text{O}$ and its preferential formation via the isotope exchange reaction between CO and C^+ .

Subject headings: ISM: abundances — ISM: molecules — molecular data — stars: individual (X Per) — ultraviolet: ISM

1. Introduction and Observations

¹Department of Physics and Astronomy, University of Toledo, Toledo, OH 43606; ysheffer@physics.utoledo.edu, sfederm@uoft02.utoledo.edu.

²Department of Astronomy, University of Texas, Austin, TX 78712; dll@astro.as.utexas.edu.

³Based on observations obtained with the NASA/ESA *Hubble Space Telescope (HST)* through the Space Telescope Science Institute, which is operated by the Association of Universities for Research in Astronomy, Inc., under NASA contract NAS5-26555.

Carbon monoxide is the second most abundant molecule in interstellar clouds after H_2 , with readily observable electronic transitions in the vacuum ultraviolet (VUV), vibrational bands in the infrared, and pure rotational lines in the mm-wave regime. The isotopic varieties of CO are used to constrain models of star formation, chemical networks, and stellar evolution. The first VUV detection of rotationally unresolved fourth-positive ($A\ ^1\Pi-X\ ^1\Sigma^+$) absorption bands from interstellar $^{12}\text{C}^{16}\text{O}$ and $^{13}\text{C}^{16}\text{O}$ was reported by Smith & Stecher (1971)—see Morton & Noreau (1994) for an extensive review of the fourth-positive bands. However, most measurements of various CO species come from radio observations of molecular clouds with substantial total column densities (N) of CO. Penzias et al. (1972) reported the first mm observations of $^{12}\text{C}^{16}\text{O}$ and $^{13}\text{C}^{16}\text{O}$ in dark clouds. Rarer CO varieties were reported later: $^{12}\text{C}^{18}\text{O}$ by Mahoney, McCutcheon, & Shuter (1976), $^{12}\text{C}^{17}\text{O}$ by Dickman et al. (1977), and $^{13}\text{C}^{18}\text{O}$ by Langer et al. (1980). The “final” milestone for radio CO was recently reached by Bensch et al. (2001), who reported the detection of the rarest stable CO isotopomer, $^{13}\text{C}^{17}\text{O}$, in the ρ Oph molecular cloud. In the VUV, absorption from CO is sought, but such observations sample substantially smaller $N(\text{CO})$ than are commonly observed in the radio because ultraviolet extinction limits the number of suitable targets behind molecular clouds. Individual $A-X$ rotational lines of interstellar absorption bands have been fully resolved and measured only for $^{12}\text{C}^{16}\text{O}$ and $^{13}\text{C}^{16}\text{O}$, using the echelle grating of the Goddard High-Resolution Spectrograph (GHRS) on board the *HST* (Smith et al. 1991; Sheffer et al. 1992). A previous detection with a GHRS first-order grating of rotationally unresolved $^{12}\text{C}^{18}\text{O}$ was reported by Lambert et al. (1994) toward ζ Oph.

In this Letter we report the first VUV detection of interstellar absorption from $^{12}\text{C}^{17}\text{O}$ bands, and present the first unblended measurements of its sibling, $^{12}\text{C}^{18}\text{O}$. These observations were made toward X Per (HD 24534), using grating E140H of the Space Telescope Imaging Spectrograph (STIS) for data sets o64812010–030 and o64813010–020. The star was observed through the smallest aperture ($0.1'' \times 0.025''$, the “Jenkins slit”), providing the highest *HST* resolving power of $\lambda/\Delta\lambda = 200,000$ over $\lambda = 1316$ to $1517\ \text{\AA}$. We modeled the data using our unpublished spectrum synthesis code, ISMOD, which is based on the line transfer equations given by Black & van Dishoeck (1988). For more details of data extraction and modeling, see Sheffer, Federman, & Lambert (2002). In the next section we present CO column densities along the X Per line of sight, and in §3 we compare CO isotopomeric ratios with ambient carbon and oxygen isotopic ratios in the context of theoretical models of translucent clouds.

2. Column Densities of CO Isotopomers

With the help of optically thin intersystem bands of CO, we derived $N(^{12}\text{C}^{16}\text{O}) = 1.41 (\pm 0.22) \times 10^{16} \text{ cm}^{-2}$ toward X Per from the same data sets used here, i.e., a column density 5.5 ± 0.9 times higher than toward ζ Oph (Sheffer et al. 2002). The column density of the $^{13}\text{C}^{16}\text{O}$ isotopomer was modeled in the same study to be $1.94 (\pm 0.08) \times 10^{14} \text{ cm}^{-2}$ by analysis of its weak $A-X(8-0)$ band. Although the column densities of the rarer isotopomers are derived below by using the same 4-cloud model, the resulting abundances of these species are sensitive only to the total equivalent width (W_λ) of each band, because the optical depth (τ) at line center is less than 1.

Rotational structures of four $^{12}\text{C}^{18}\text{O}$ $A-X$ bands are now resolved: see (2–0), (3–0), (4–0), and (5–0) in Figure 1. Table 1 lists their laboratory wavelengths computed from term values given by Beaty et al. (1997), who measured VUV emission line positions for $v' = 0$ to 9 at $R = 130,000$. The match of laboratory wavelengths with observed positions of X Per absorption lines is very good, i.e., they are consistent with the radial velocity of CO along this line of sight. Electric dipole oscillator strengths (f -values) are normally assumed to be identical for all CO isotopomers. Therefore, $N(^{12}\text{C}^{18}\text{O})$ was derived by fitting the position and strength of observed bands using published f -values of $^{12}\text{C}^{16}\text{O}$ (Chan, Cooper, & Brion 1993). For the group of four $A-X$ bands modeled here together, their average f -value taken from Chan et al. (1993) is only 3.5% smaller than an average based on f -values recommended by Eidelsberg et al. (1999). Values of band W_λ and $\tau[R(0)]$ are also listed in Table 1 to show that these rare species indeed have optically thin lines. All four bands were fitted simultaneously, to increase the “signal-to-noise ratio” of the model. In a complementary manner, individual band fits are used to derive formal error bars for modeled parameters.

The column density of $^{12}\text{C}^{18}\text{O}$ is found to be $4.69 (\pm 0.66) \times 10^{12} \text{ cm}^{-2}$. Another free fitting parameter, the ground state excitation temperature ($T_{J''>0, J''=0}$), is consistent with very low rotational temperatures usually found in the VUV for CO in diffuse clouds: $T_{1,0}(^{12}\text{C}^{18}\text{O}) = 3.4 (\pm 1.0) \text{ K}$. For comparison, we find $T_{1,0} = 3.3 \text{ K}$ and 3.7 K from the $A-X(8-0)$ bands of $^{12}\text{C}^{16}\text{O}$ and $^{13}\text{C}^{16}\text{O}$, respectively, toward X Per. For the $J'' = 2$ rotational level, we provide a 2σ upper limit, $T_{2,0} \leq 6.2 \text{ K}$.

Identical steps of observational reductions and data modeling were followed with spectral segments of $^{12}\text{C}^{17}\text{O}$ bands, although rest wavelengths had to be computed indirectly from $^{12}\text{C}^{16}\text{O}$ molecular constants, see Table 1. Figure 1 presents fits of the four $A-X$ bands of $^{12}\text{C}^{17}\text{O}$: (2–0), (3–0), (4–0), and (5–0). The measured column density of $^{12}\text{C}^{17}\text{O}$ is $1.63 (\pm 0.62) \times 10^{12} \text{ cm}^{-2}$. A reliable determination of $T_{1,0}$ was possible only from the (3–0) band, on account of the extreme weakness of the $^{12}\text{C}^{17}\text{O}$ $J'' > 0$ lines. Thus $T_{1,0}(^{12}\text{C}^{17}\text{O}) = 3.1 (\pm$

2.0) K, where twice the uncertainty from the four-band C¹⁸O model is adopted for this one-band result. Note that the $X^1\Sigma^+$ (ground state) rotational levels of ¹²C¹⁷O are intrinsically split into hyperfine components, observable as radio line separations of $\sim 3 \text{ km s}^{-1}$ or less (see Figure 1 of Bensch et al. 2001). Furthermore, since $A^1\Pi$ hyperfine splittings should be much smaller than ground state splittings, hyperfine separations for VUV transitions are of the order of $10^{-4} \text{ km s}^{-1}$, which we ignore here.

3. CO Isotopomeric Ratios toward X Per

As described in the last section, column densities for four CO isotopomers toward X Per are now available from STIS spectra of $A-X$ bands. Note that VUV absorptions are confined to the narrow beam subtended by the background star, whereas radiotelescopes that are used for emission measurements have much larger beam sizes. Of particular diagnostic value are the isotopomeric column density ratios and their departures from ambient isotopic ratios. In Table 2 we list CO isotopomeric ratios derived from our data, as well as carbon and oxygen isotopic ratios that were measured for local molecular clouds and are taken from reviews by Wilson & Rood (1994) and Wilson (1999). The galactocentric distance of X Per is 9% larger than that of the Sun; we assume that the material along its sight line is represented by local ISM abundances. The level of isotopic fractionation is given by $F \neq 1$, where F is defined as the isotopomeric ratio normalized by the corresponding isotopic ratio. From Table 2 we get $F(12,13) \equiv (^{12}\text{C}^{16}\text{O}/^{13}\text{C}^{16}\text{O})/(^{12}\text{C}/^{13}\text{C}) = 1.0 \pm 0.2$, $F(16,18) = 5.4 \pm 1.2$, $F(16,17) = 4.6 \pm 1.9$, and $F(18,17) = 0.9 \pm 0.4$. Relative to ¹²C¹⁶O, the ¹³C¹⁶O isotopomer is unfractionated. Both ¹²C¹⁸O and ¹²C¹⁷O are quite severely fractionated but by similar factors such that $F(18,17)$ is consistent with unity within the errors of measurement.

The line of sight through the translucent (Snow et al. 1998, $A_V \approx 1.44 \text{ mag}$) cloud toward X Per harbors a total CO column density of $1.43 \times 10^{16} \text{ cm}^{-2}$, which is one of the larger values observed in the VUV to date, but certainly is much smaller (by 1 to 3 orders of magnitude) than column densities commonly observed via radio emission in molecular clouds. CO photochemistry in diffuse and translucent clouds has been studied theoretically in many papers, e.g., van Dishoeck & Black (1988) and Warin, Benayoun, & Viala (1996). The equilibrium CO abundance is dependent in large part on photodissociation driven by absorption of ultraviolet photons in bound-bound transitions to excited states from which predissociation occurs. Multiple electronic transitions are involved in the dissociation. Calculation of the photodissociation rate depends, of course, on the adopted interstellar radiation field, I_{UV} , and the penetration of the ultraviolet photons into a cloud. This latter process is affected by the ultraviolet opacity of the embedded dust grains and by τ in the

CO “photodissociating” lines and in overlapping H₂ and H Lyman lines. When τ of such key lines is large, CO molecules become shielded against I_{UV} . Self-shielding may occur for transitions not overlapped by hydrogen absorption.

All CO isotopomers are subject to photodissociation, the rate of which, Γ_i (where i stands for an isotopomeric flavor), decreases into the cloud as molecular abundances and their opacities (and that from grains) build up. As a natural outcome of the preponderance of ¹²C and ¹⁶O among all carbon and oxygen isotopes, the primary isotopomer of CO is subject to greater self-shielding, resulting in a steeper gradient of growing abundance into the cloud. For unshielded CO molecules, e.g., at the edge of a cloud, the photodissociation rates of the various isotopomers are at their maximum values and effectively identical. Owing to wavelength shifts between the “photodissociating” transitions of different isotopomers, the dominant molecule ¹²C¹⁶O cannot fully self-shield the less abundant isotopomers. Indeed, Warin et al. (1996) describe the shielding of rare isotopomers by ¹²C¹⁶O as “not efficient”. Calculations show that ¹²C¹⁶O can be shielded from the ultraviolet over a large portion of a diffuse or translucent cloud but trace species like ¹²C¹⁸O are almost entirely unshielded. Therefore, the faster build up of ¹²C¹⁶O with depth into the cloud is predicted to be manifested in increased fractionation because, e.g., $F(16,18) = \Gamma_{1218}/\Gamma_{1216} > 1$.

In diffuse and translucent clouds, carbon is predominantly ionized (Sofia, Fitzpatrick, & Meyer 1998). Consequently, the behavior of $F(12,13)$ is compounded by the isotope exchange reaction (Watson, Anicich, & Huntress 1976), $^{13}\text{C}^+ + ^{12}\text{C}^{16}\text{O} \leftrightarrow ^{13}\text{C}^{16}\text{O} + ^{12}\text{C}^+ + \Delta E (= 34.6 \text{ K})$, which is very competitive with the photodissociation rate Γ_{1316} because its rate coefficient k_f is $6.8 \times 10^{-10} \text{ cm}^3 \text{ s}^{-1}$ (Smith & Adams 1980, at $T = 80 \text{ K}$), and which is able, therefore, to enhance the abundance of ¹³C-containing isotopomers at the expense of ¹²C-containing isotopomers. (An analogous isotope exchange reaction involving oxygen ions, working to reduce both $F(16,18)$ and $F(16,17)$, is inhibited by the fact that oxygen is predominantly neutral in these environments.) The outcome for ¹³C¹⁶O is a compromise between the two isotope selective processes, photodissociation and isotope exchange. Indeed, published photochemical models (see more below) do show that $F(12,13)$ is expected to be ~ 1 in the outer cloud envelope even though $\Gamma_{1316}/\Gamma_{1216} > 1$, and remain ~ 1 until the interior parts of the cloud are reached, where photodissociation suffers great extinction and where CO becomes the most abundant form of carbon instead of C⁺, thus extinguishing the isotope exchange reaction.

Qualitatively, our measured isotopomeric ratios fit the above description of CO photochemistry in translucent clouds. First, the ¹²C¹⁶O/¹³C¹⁶O ratio is equal to the ambient carbon isotopic ratio. Since Γ_{1316} is expected to be significantly higher than Γ_{1216} , the isotope exchange reaction must be operating in the probed regions of the clouds to effectively

reduce $F(12,13)$ from ≈ 5.4 , the value of $F(16,18)$, to 1. (The similarity of Γ_{1316} and Γ_{1218} is predicted by the similarity of the shielding functions of the two isotopomers, as can be seen in Table 5 of van Dishoeck & Black 1988.) A different interpretation, that of a fully efficient shielding for both species, must imply that the isotope exchange reaction is not operating. Such a scenario is possible only for a warm cloud with $T_{\text{kin}} \gtrsim 160$ K, a value much higher than 20 K, as was inferred from a chemical model of the X Per line of sight (Federman et al. 1994). Second, both trace species $^{12}\text{C}^{17}\text{O}$ and $^{12}\text{C}^{18}\text{O}$ are underabundant relative to $^{12}\text{C}^{16}\text{O}$ by a factor of ~ 5 . This suggests that neither trace species is significantly shielded. An inspection of the van Dishoeck & Black (1988) translucent cloud models, especially using their Fig. 11 of cumulative column densities ratios from model T6, shows that $F(16,18)$ does, indeed, climb up to ~ 5 some 1 pc into the cloud, where $A_V \sim 1.2$ mag from cloud edge. Simultaneously, the value of $F(12,13)$ remains close to 1 throughout the cloud, because both isotope selective processes very nearly cancel each other.

Unfortunately, CO column densities obtained from Table 5 of van Dishoeck & Black (1988) do not agree with our observed values, in the sense that in order to reproduce observed isotopomeric ratios, one has to pick those models with $N(\text{CO})$ much higher than observed. Specifically, models T2 and H3 have values of A_V , $N(\text{H}_2)$, $N(\text{C}^+)$, and $N(^{12}\text{C}^{16}\text{O})$ that match the X Per line of sight. However, the same models display values for $F(12,13)$ and $F(16,18)$ that are some 50% smaller than our observed values. On the other hand, whereas our isotopomeric ratios are matched by CO ratios from models T4, H4, and H5, the corresponding modeled CO column densities for all isotopomers are 10 to 40 times higher than observed values. In fact, the high- $N(\text{CO})$ discrepancy is highlighted by the persistent agreement between modeled and observed $N(\text{C}^+)$ values. Part of the discrepancy may be due to the X Per line of sight passing through the cloud envelope, but not through the cloud center. Such a scenario has been explored by Kopp, Roueff, & Pineau des Forêts (2000), who showed that CO (but not C^+) is especially sensitive to model geometry. In particular, for the same total extinction, off-center optical paths through a spherical cloud can generate $N(\text{CO})$ values lower by 1 to 2 orders of magnitude than values from a path that is perpendicular to a plane-parallel slab, the likes of which were employed by van Dishoeck & Black (1988) and by Warin et al. (1996). Interestingly, Snow et al. (1998) suggested that the cloud toward X Per might be a dispersing remnant of a denser molecular cloud. Besides not resembling a plane-parallel slab, this cloud may also pose modeling difficulties in terms of unsatisfied steady-state assumptions.

Likewise, it is possible to find partial agreement between the single, $A_V = 4.34$ mag model of a translucent cloud from Warin et al. (1996) and our results. As abundances of all CO species increase into the cloud owing to enhanced UV shielding (see their Figure 7), both $^{12}\text{C}^{16}\text{O}$ and $^{13}\text{C}^{16}\text{O}$ first reach a plateau at $A_V \sim 1.0$, where their mutual ratio is

~ 70 , or $F(12,13) \sim 0.8$, since their input carbon isotopic ratio is 90. Furthermore, at that very point into the cloud, the ratio of $^{12}\text{C}^{16}\text{O}$ to $^{12}\text{C}^{18}\text{O}$ stands at ~ 2000 , i.e., $F(16,18) \sim 4$. But in a similar fashion to the models of van Dishoeck & Black (1988), predicted $N(\text{CO})$ values are more than 10 times higher than those observed toward X Per. Warin et al. (1996) also modeled individual rotational level populations for the CO isotopomers, since level photodissociation rates are coupled to ground state excitation temperatures. Modeled $T_{J''>0, J''=0}$ values are higher than our observed values, with $T_{1,0} \sim 0.1 \times T_{\text{kin}} \sim 5$ K. One possible remedy is to assume that the same ratio of $T_{1,0}$ over T_{kin} applies to the X Per clouds. In that case, the observed $T_{1,0}$ value of ≈ 3.5 K may indicate that T_{kin} is ≈ 35 K toward X Per, rather than 20 K. Indeed, Kaczmarczyk (2000) derived $T_{\text{kin}} = 45 (\pm 15)$ K from observations of C_2 along this line of sight.

4. Concluding Remarks

The line of sight toward X Per has provided us with a rich spectrum of $A-X$ bands of CO, allowing the first VUV detection of the rare isotopomer $^{12}\text{C}^{17}\text{O}$ and the first rotationally-resolved views of both $^{12}\text{C}^{18}\text{O}$ and $^{12}\text{C}^{17}\text{O}$. These detections were made possible by the superb qualities of STIS as a VUV spectrometer. Toward X Per we find that $^{13}\text{C}^{16}\text{O}$ is unfractionated with respect to $^{12}\text{C}^{16}\text{O}$ owing to a balance between the rates of photodissociation and of the isotope exchange reaction. On the other hand, the lack of an isotope exchange reaction in the case of oxygen isotopes renders both $^{12}\text{C}^{18}\text{O}$ and $^{12}\text{C}^{17}\text{O}$ strongly fractionated and destroyed at the 80% level with respect to the strongly shielded $^{12}\text{C}^{16}\text{O}$. As was described above, similar isotopomeric ratios are to be found within published results from theoretical models. However, a large gap remains between observed and modeled column densities for CO.

With the detection of $^{12}\text{C}^{17}\text{O}$ toward X Per, observers of interstellar absorption lines are left with the last two stable CO isotopomers that have yet to be detected in the ultraviolet, namely, $^{13}\text{C}^{18}\text{O}$ and $^{13}\text{C}^{17}\text{O}$. These are very challenging tasks at best, as the respective intrinsic abundances are expected to be $\frac{1}{24}$ and $\frac{1}{70}$ the abundance of $^{12}\text{C}^{17}\text{O}$. Whereas $^{13}\text{C}^{18}\text{O}$ was included in models of translucent clouds, not even a coarse grid of theoretical models exists for $^{12}\text{C}^{17}\text{O}$ in translucent clouds. Hopefully, the new observations of this species as reported here and of $^{13}\text{C}^{17}\text{O}$ by Bensch et al. (2001) will provide an incentive for the inclusion of ^{17}O -bearing molecules in computer simulations. There is also a need for laboratory measurements, since the $A-X$ bands of $^{12}\text{C}^{17}\text{O}$ currently lack rigorous wavelength and perturbation analyses.

We thank an anonymous referee for very rapid handling of this manuscript. The research presented here was supported in part by a NASA grant for *HST* program GO-08622 and NASA grant NAG5-4957 to the University of Toledo.

REFERENCES

- Beatty, L. M., Braun, V. D., Huber, K. P., & Le Floch, A. C. 1997, *ApJS*, 109, 269
- Bensch, F., Pak, I., Wouterloot, J. G. A., Klapper, G., & Winnemisser, G. 2001, *ApJ*, 562, L185
- Black, J. H., & van Dishoeck, E. F. 1988, *ApJ*, 331, 986
- Chan, W. F., Cooper, G., & Brion, C. E. 1993, *Chem. Phys.*, 170, 123
- Dickman, R. L., Langer, W. D., McCutcheon, W. H., & Shuter, W. L. H. 1977, in *CNO Isotopes in Astrophysics*, ed. J. Adouze (Dordrecht: Reidel), 95
- Eidelsberg, M., Jolly, A., Lemaire, J. L., Tchang-Brillet, W.-Ü. L., Breton, J., & Rostas, F. 1999, *A&A*, 346, 705
- Federman, S. R., Strom, C. J., Lambert, D. L., Cardelli, J. A., Smith, V. V., & Joseph, C. L. 1994, *ApJ*, 424, 772
- Kaczmarczyk, G. 2000, *Acta Astron.*, 50, 151
- Kopp, M., Roueff, E., & Pineau des Forêts, G. 2000, *MNRAS*, 315, 37
- Lambert, D. L., Sheffer, Y., Gilliland, R. L., & Federman, S. R. 1994, *ApJ*, 420, 756
- Langer, W. D., Goldsmith, P. F., Carlson, E. R., & Wilson, R. W. 1980, *ApJ*, 235, L39
- Mahoney, M. J., McCutcheon, W. H., & Shuter, W. L. H. 1976, *AJ*, 81, 508
- Morton, D. C., & Noreau, L. 1994, *ApJS*, 95, 301
- Penzias, A. A., Solomon, P. M., Jefferts, K. B., & Wilson, R. W. 1972, *ApJ*, 174, L43
- Sheffer, Y., Federman, S. R., & Lambert, D. L. 2002, *ApJ*, 572, L95
- Sheffer, Y., Federman, S. R., Lambert, D. L., & Cardelli, J. A. 1992, *ApJ*, 397, 482
- Smith, A. M., & Stecher, T. P. 1971, *ApJ*, 164, L43

Smith, A. M., et al. 1991, ApJ, 377, L61

Smith, D., & Adams, N. G. 1980, ApJ, 242, 424

Snow, T. P., Hanson, M. M., Black, J. H., van Dishoeck, E. F., Crutcher, R. M., & Lutz, B. L. 1998, ApJ, 496, L113

Sofia, U. J., Fitzpatrick, E. L., & Meyer, D.M. 1998, ApJ, 504, L47

van Dishoeck, E. F., & Black, J. H., 1988, ApJ, 334, 771

Warin, S., Benayoun, J. J., & Viala, Y. P. 1996, A&A, 308, 535

Watson, W. D., Anicich, V. G., & Huntress, W. T. Jr. 1976, ApJ, 205, L165

Wilson, T. L. 1999, Rep. Prog. Phys. 62, 143

Wilson, T. L., & Rood, R. T. 1994, ARA&A, 32, 191

Table 1. Rare Species of CO toward X Per

$A-X$	$^{12}\text{C}^{18}\text{O}$				$^{12}\text{C}^{17}\text{O}$			
	(2-0)	(3-0)	(4-0)	(5-0)	(2-0)	(3-0)	(4-0)	(5-0)
$\lambda_0[R(1)]$ (Å)	1478.845	1449.248	1421.487	1395.416	1478.219	1448.332	1420.320	1394.029
$\lambda_0[R(0)]$ (Å)	1478.895	1449.294	1421.530	1395.455	1478.270	1448.379	1420.363	1394.069
$\lambda_0[Q(1)]$ (Å)	1478.975	1449.371	1421.604	1395.526	1478.352	1448.458	1420.439	1394.142
v_{helio} (km s $^{-1}$)	14.8	15.0	14.4	15.9	13.8	13.5	13.4	13.5
W_λ (mÅ)	3.14 ± 0.26	2.65 ± 0.17	1.84 ± 0.23	1.10 ± 0.14	1.22 ± 0.21	1.02 ± 0.14	0.69 ± 0.17	0.40 ± 0.17
$\tau[R(0)]$	0.6	0.5	0.4	0.2	0.2	0.2	0.1	0.1

Note. — Laboratory wavenumbers for $^{12}\text{C}^{18}\text{O}$ were calculated from the term values of Beaty et al. (1997). Wavenumbers for $^{12}\text{C}^{17}\text{O}$ were computed from Dunham coefficients for $^{12}\text{C}^{16}\text{O}$ (corrected by the proper reduced-mass factors) and then shifted to correct for $^{12}\text{C}^{18}\text{O}$ wavenumber differences between our inferred values and those of Beaty et al. (1997). Although such shifts were not larger than 0.16 cm^{-1} (3 mÅ), the apparent velocity difference of 1.4 km s^{-1} (7 mÅ) between the two species indicates that a possible systematic shift may be affecting our computed $^{12}\text{C}^{17}\text{O}$ wavenumbers.

Table 2. Isotopic Comparisons toward X Per

Isotopomeric Ratios	Local Isotopic Ratios
$\frac{N(^{12}\text{CO})}{N(^{13}\text{CO})} = 73 \pm 12$	$\frac{^{12}\text{C}}{^{13}\text{C}} = 70 \pm 7$
$\frac{N(\text{C}^{16}\text{O})}{N(\text{C}^{18}\text{O})} = 3000 \pm 600$	$\frac{^{16}\text{O}}{^{18}\text{O}} = 560 \pm 25$
$\frac{N(\text{C}^{16}\text{O})}{N(\text{C}^{17}\text{O})} = 8700 \pm 3600$	$\frac{^{16}\text{O}}{^{17}\text{O}} = 1900 \pm 200$
$\frac{N(\text{C}^{18}\text{O})}{N(\text{C}^{17}\text{O})} = 2.9 \pm 1.2$	$\frac{^{18}\text{O}}{^{17}\text{O}} = 3.4 \pm 0.2$

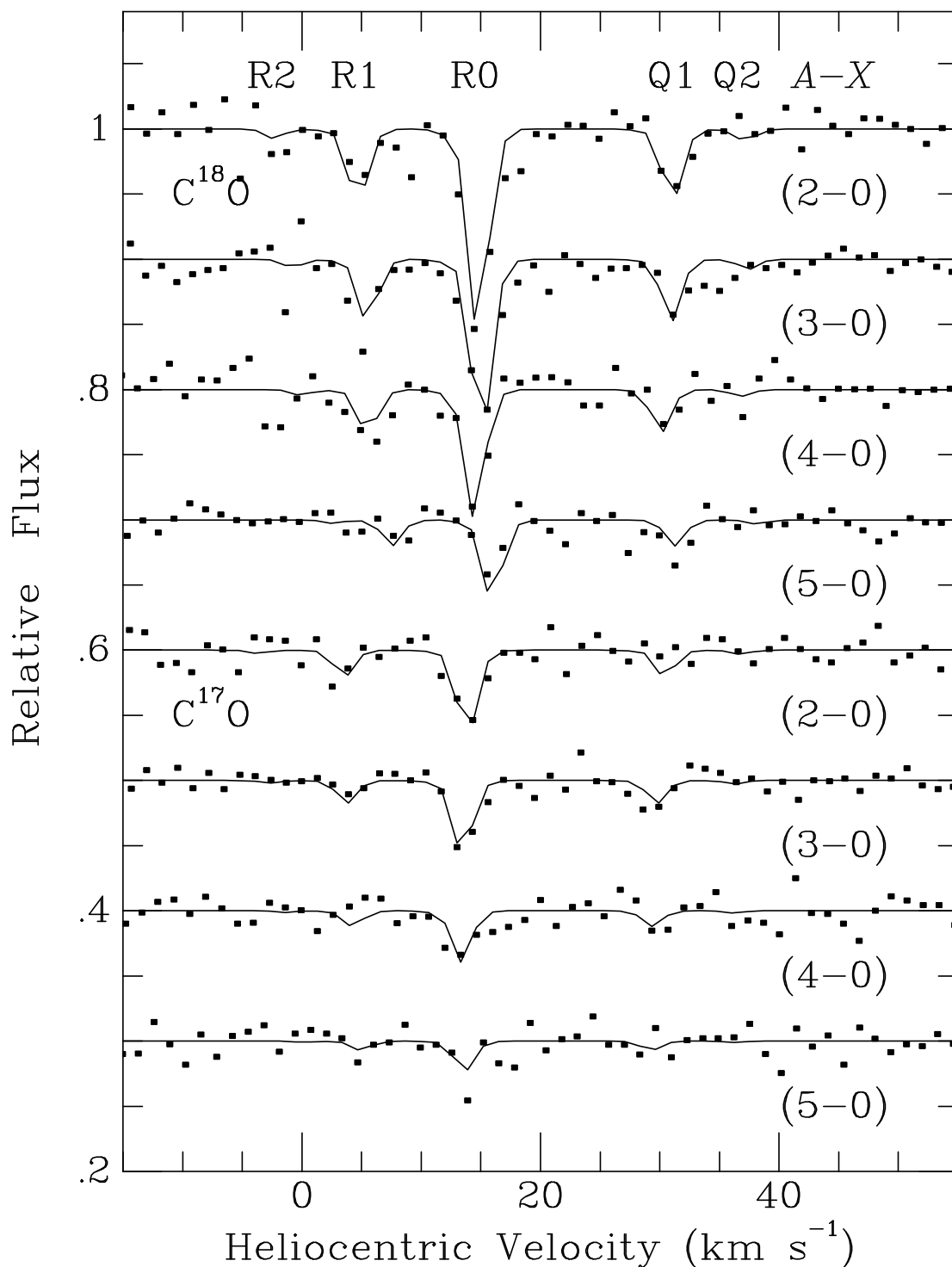


Fig. 1.— Montage of four $A-X$ bands of $^{12}\text{C}^{18}\text{O}$ and four $A-X$ bands of $^{12}\text{C}^{17}\text{O}$. STIS data toward X Per are shown as filled squares, while global models are shown by solid lines. Both data and models have been rebinned by two for clarity. The heliocentric radial velocity is shown for the $R(0)$ line of all bands, which are shifted by -0.1 in continuum units.